Transport Properties of an Electron-Hole Bilayer in Contact with a Superconductor Hybrid Junction

D. Bercioux,[1,2,*] T. M. Klapwijk,[4] and F. S. Bergeret[1,3,†]
[1]Donostia International Physics Center (DIPC), Manuel de Lardizbal 4, E-20018 San Sebastián, Spain
[2]IKERBASQUE, Basque Foundation of Science, 48011 Bilbao, Basque Country, Spain
[3]Centro de Física de Materiales (CFM-MPC) Centro Mixto CSIC-UPV/EHU, 20018 Donostia-San Sebastian, Basque Country, Spain
[4]Kavli Institute of Nanoscience, Delft University of Technology, Lorentzweg 1, 2628 CJ Delft, The Netherlands
(Received 30 March 2017; published 7 August 2017)

We investigate the transport properties of a junction consisting of an electron-hole bilayer in contact with normal and superconducting leads. The electron-hole bilayer is considered as a semimetal with two electronic bands. We assume that in the region between the contacts the system hosts an exciton condensate described by a BCS-like model with a gap Γ in the quasiparticle density of states. We first discuss how the subgap electronic transport through the junction is mainly governed by the interplay between two kinds of reflection processes at the interfaces: the standard Andreev reflection at the interface between the superconductor and the exciton condensate, and a coherent crossed reflection at the semimetal–exciton-condensate interface that converts electrons from one layer into the other. We show that the differential conductance of the junction shows a minimum at voltages of the order of Γ/e. Such a minimum can be seen as a direct hallmark of the existence of the gapped excitonic state.

DOI: 10.1103/PhysRevLett.119.067001

Introduction.—Semimetals (SMs) could undergo, at sufficiently low temperatures, a phase transition into an insulating state described by electron-hole bound pairs. These pairs form a so-called exciton condensate (EC), as theoretically predicted a long time ago [1–3]; one refers to the system being in an excitonic insulating phase. The ground state of such a phase can be described with the help of a BCS-like theory, in analogy with the superconducting phase. However, the coupling strength in an excitonic insulator is expected to be even weaker than in a superconductor (S). Furthermore, electron-hole recombination can be quite fast, thereby preventing the formation of the condensate. For these reasons the EC remains an elusive phase of matter [1,2,4]. Possible SM candidates suggested to undergo a transition to the excitonic insulating phase with an EC are transition-metal dichalcogenide $TiSe_2$ [5,6] and HgTe quantum well with a thickness of 20 nm [7–9]. However, there is no conclusive evidence for an EC in such systems. So far, the most successful attempt to obtain an EC is based on the condensation of excitons coupled to light confined within CdTe/CdMgTe microcavities—the so-called exciton polaritons [10].

In addition to bulk semimetals, there have been several proposals to create an EC in systems with spatially separated electron and hole gases in order to reduce the electron-hole recombination rate. The exciton formation in such electron-hole bilayers can be detected by Coulomb drag measurements [11–16]. According to the theory, if the excitons form a condensate, one expects a discontinuity in the drag at the critical temperature and a divergence when $T \to 0$ [17]. Although certain anomalies of the Coulomb drag as a function of temperature have been observed [11,12], it is hard to attribute them to the formation of an exciton condensate.

The primary motivation of this Letter is to propose and explore an additional type of measurements to validate the existence of an EC in electron-hole bilayers. Instead of measuring the Coulomb drag, we suggest to perform a differential conductance measurement using normal and superconducting electrodes (see Fig. 1), to directly unveil the presence of the excitonic gap. We show that the transport at low voltages is determined by the competition between the intralayer Andreev reflection and the interlayer normal reflection between the SM and the EC parts of the system. The latter process is analogous to the one introduced by Rontani and Sham for direct SM-EC interfaces [18–20].

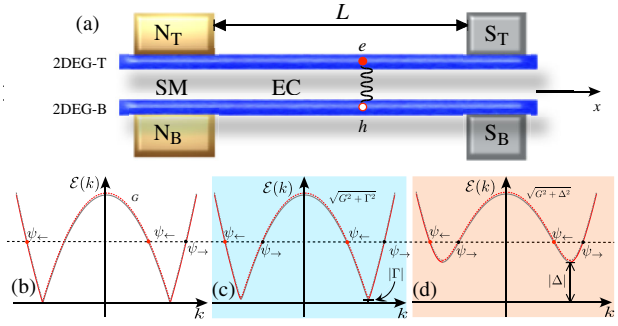

FIG. 1. (a) Sketch of the electron-hole bilayer with the two normal ($N_{T/B}$) and two superconducting electrodes ($S_{T/B}$); the EC region in the middle has length L. Energy spectra are shown for the SM region (b), the EC region (c), and the SSM region (d).

We discuss the competition between these two types of reflections as a function of the length of the EC region and show that this competition leads to a minimum of the full differential conductance at a voltage V_0 of the order of the EC order parameter.

Model and formalism.—We consider an ideal two-dimensional electron-hole bilayer, characterized by two parallel two-dimensional electron gases with opposite particle filling, as illustrated in Fig. 1(a): the top layer (TL) is "electron doped" whereas the bottom layer (BL) is "hole doped." By gating the two layers independently it is possible to modulate the band overlap G between the bands of the TL and BL [21]. We assume a spatial modulation along the x axes of the Coulomb interaction in the electron-hole bilayer. In the parts of the bilayer covered by the metallic electrodes, the charge screening allows for the neglecting of the Coulomb interaction. Thus, the left and right parts of the system are described by a SM consisting of two bands—one from each layer—crossing at the Fermi level [see Fig. 1(a)]. Because of the proximity effect, we assume an induced superconducting gap Δ on the part of the layers below the S contacts [see Fig. 1(c)]. In the region between the contacts, the reduced screening results in an indirect EC described by the order parameter Γ [21] [see Fig. 1(b)].

To be precise, the structure shown in Fig. 1(a) is modeled as a SM, i.e., $\Gamma = \Delta = 0$, in contact with a central region of length L with a finite EC coupling ($\Gamma \neq 0$ and $\Delta = 0$). In the region $x > L$ we assume $\Delta \neq 0$ due to the proximity from the S electrodes [22] and $\Gamma = 0$. We denote this region as SSM (superconducting proximitized semi-metal). This junction is described by the following Hamiltonian written in an extended Nambu space [23]:

$$\mathcal{H}_{\mathrm{Hyb}} = \begin{pmatrix} \boldsymbol{p}^2/2m - G & \Gamma(x) & \Delta(x)e^{i\phi} & 0 \\ \Gamma(x)^* & G - \boldsymbol{p}^2/2m & 0 & \Delta(x)e^{i\phi} \\ \Delta(x)e^{-i\phi} & 0 & G - \boldsymbol{p}^2/2m & -\Gamma(x) \\ 0 & \Delta(x)e^{-i\phi} & -\Gamma(x)^* & \boldsymbol{p}^2/2m - G \end{pmatrix}, \tag{1}$$

where

$$\Gamma(x) = \Gamma\Theta(x)(1 - \Theta(x - L)), \tag{2a}$$

$$\Delta(x) = \Delta\Theta(x - L), \tag{2b}$$

and $\Theta(x)$ is the Heaviside step function. The Hamiltonian (1) is written in the basis defined by the *bi* spinor $\Psi = (\psi_{\mathrm{TL},\sigma}, \psi_{\mathrm{BL},\sigma}, \psi^\dagger_{\mathrm{TL},-\sigma}, \psi^\dagger_{\mathrm{BL},-\sigma})$, where σ is the spin [23,24]. We account for possible elastic reflection at the SM-EC and EC-SSM interfaces by introducing delta barriers in the system Hamiltonian [25], $\mathcal{H}_{\mathrm{int}} = H_{\text{SM-EC}}\delta(x) + H_{\text{EC-SSM}}\delta(x - L)$. This reflection can be ascribed, for example, to the mismatch of the Fermi wave vector in the different regions [26].

We analyze the scattering properties of this hybrid SM-EC-SSM junction by matching the scattering states at each interface separating these three regions [27]. In the SM region, there is no coupling between the TL and BL nor between electron and hole of the same layer. Thus, we can consider an electron (hole) in the TL (BL) as an initial scattering state. In the middle, EC, region, there is a finite coupling between electrons of TL and BL proportional to Γ. In the SSM region, the superconducting pairing Δ couples electrons and holes within the same layer.

We summarize all possible processes that an incoming electron from the TL of the SM at energies smaller than Γ and Δ may experience. If we look at the SM-EC interface, the electron can be either normal reflected in the same layer with amplitude, $r_{N,T\to T} \equiv r_{NTT}$, or in the opposite layer, $r_{N,T\to B} \equiv r_{NTB}$. The latter process resembles the Andreev reflection at the $S - N$ interface and was studied by Rontani and Sham in Refs. [18–20]. It results in an exciton in the EC region, whereas at the EC-SSM interface the electron can be Andreev reflected into a hole either in the same layer, $r_{A,T\to T} \equiv r_{ATT}$, or into the other layer, $r_{A,T\to B} \equiv r_{ATB}$. It is interesting to notice that the reflection amplitude r_{ATB} is the analog to the Andreev specular reflection in Dirac-material–superconductor hybrid junctions [22].

For energies higher than the EC gap, $\mathcal{E} > |\Gamma|$, the particles travel through the EC region as propagating waves. In contrast, for $\mathcal{E} < |\Gamma|$, the quasibound states are characterized by complex momenta describing evanescent modes. The characteristic decay length of these modes ξ_Γ is energy dependent and given by

$$\xi_\Gamma^{-1} = \sqrt{\frac{1}{2}\left(\chi_Q + \sqrt{\chi_Q^2 + \frac{4m^2}{\hbar^4}(\Gamma^2 - \mathcal{E}^2)}\right)}, \tag{3}$$

where $\chi_Q = Q^2 - 2mG/\hbar^2$; here, Q is the momentum parallel to the interfaces that is conserved in the scattering process [27]. When the band overlap G is the dominant energy scale, i.e., $G \gg \max[\Gamma, \Delta, \mathcal{E}]$, the EC characteristic length scale is approximated by

$$\xi_\Gamma = \frac{4\hbar\sqrt{mG^3}}{\Gamma(4mG + Q^2\hbar^2)}. \tag{4}$$

In what follows, we focus on the subgap transport; i.e., we consider the injection of electrons from the TL with

energies smaller than the SSM gap, $\mathcal{E} < |\Delta|$. Furthermore, we also assume that $\Gamma < \Delta < G$. The probability for the four possible reflection channels in the SM electrode are then given by [27]

$$R_{NTT}(\alpha) = |r_{NTT}(\alpha)|^2, \tag{5a}$$

$$R_{NTB}(\alpha) = |r_{NTB}(\alpha)|^2 \left| \frac{\mathrm{Im}[\kappa_-]}{\kappa_+}(\alpha) \right| \Theta(G - \mathcal{E}), \tag{5b}$$

$$R_{ATT}(\alpha) = |r_{ATT}(\alpha)|^2 \left| \frac{\mathrm{Im}[\kappa_-]}{\kappa_+}(\alpha) \right| \Theta(G - \mathcal{E}), \tag{5c}$$

$$R_{ATB}(\alpha) = |r_{ATB}(\alpha)|^2, \tag{5d}$$

where α is the injection angle. For angles larger than a critical $\alpha_c = \arcsin[\pm\sqrt{|G-\mathcal{E}|/\mathcal{E}+G}]$, $R_{NTB} = R_{ATT} = 0$ because of the lack of propagating states on the TL and BL. The actual form of the reflection and transmissions amplitudes are obtained by solving the scattering problem at the two interfaces [27].

Results.—We now analyze the dependence of the probabilities (5) on the length of the EC region. In the limiting case $L = 0$ the system consists of a simple SM-SSM junction. In this case, the absence of the EC leads to $r_{NTB} = 0$. Moreover, r_{ATB} also vanishes and the results for a clean interface coincide with the standard N-S junction case [25,27]. Here we stress the analogy between the interlayer Andreev reflection and the specular Andreev reflection typical of SM with Dirac spectrum again [22,29,30]. If there is no EC then electrons from the TL and BL are decoupled and, hence, all reflections occur within the same layer only.

We now focus on the more interesting case of a finite EC region, $L \neq 0$. In Fig. 2 we present the reflections R_{NTB} and R_{ATT} as a function of the injection energy and length of the EC region for a normal injection angle ($\alpha = 0$). For a length smaller than ξ_Γ, the probability for an injected electron in the TL to reach the EC-SSM interface is large. The electron is then Andreev reflected as a hole of the same layer. This explains that for small L, the Andreev reflection, R_{ATT}, dominates over the interlayer one, R_{NTB}, at all energies.

By increasing the length of the EC region, the probability to reach the EC-SSM interface for an injected electron with energy $\mathcal{E} < \Gamma$ decreases and, hence, the R_{ATT} processes are suppressed, whereas the R_{NTB} ones are enhanced. The crossover between these two behaviors depends on the injection energy. In the limiting case $L \gg \xi_\Gamma$, the probability for the injected TL electron of reaching the SSM electrode is exponentially small and the system behaves as a SM-EC junction with the reflection probability $R_{NTB} = 1$ [18,19]. For injection energies larger than the EC gap $|\Gamma|$ (but smaller than Δ), all electrons propagate towards the EC-SSM interface and, hence, Andreev processes dominate, whereas R_{NTB} decreases to zero by increasing the

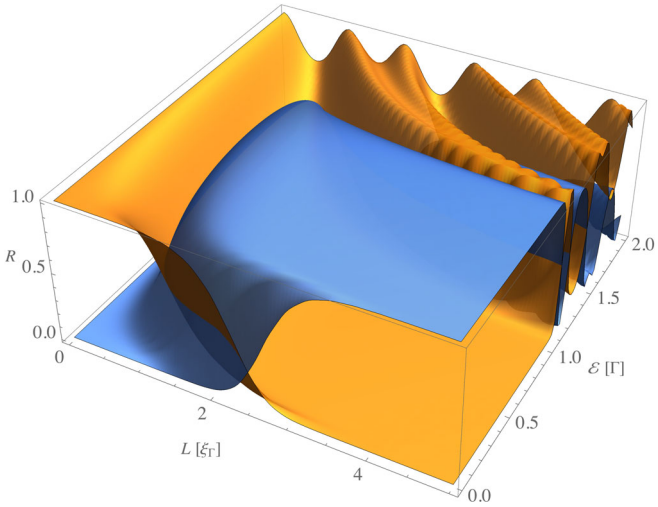

FIG. 2. R_{NTB} reflection (blue surface) and R_{ATT} (orange surface) reflection as a function of the length of EC region L and injection energy $\mathcal{E}$; both surfaces are shown for injection energies up to Δ. Here, we have used $\Gamma = 1$, $\Delta = 2\Gamma$, $G = 100\Gamma$, and normal incidence $\alpha = 0$.

injection energy. The oscillatory behavior we observe for this energy range is a feature of quasibound states in the EC region.

Analytically we can calculate the reflection probabilities (5b) and (5c) in the short-junction limit, $\delta = L/\xi_\Gamma \ll 1$, within the Andreev approximation, i.e., $G \gg \mathrm{Max}[\mathcal{E}, \Delta, \Gamma]$. In this limit and for zero injection angle $\alpha = 0$, we obtain

$$R_{NTB} = 4\delta^2 \frac{\mathcal{E}^2\Gamma^2}{\Delta^2(\Gamma^2 - \mathcal{E}^2)}, \tag{6a}$$

$$R_{ATT} = 1 - 4\delta^2 \frac{\mathcal{E}^2\Gamma^2}{\Delta^2(\Gamma^2 - \mathcal{E}^2)}, \tag{6b}$$

$$R_{NTT} = 0. \tag{6c}$$

These expressions are in agreement with the numerical results shown in Fig. 2 within the small-L region. Notice that for the large value of G chosen, $G = 100\Gamma$, the probability for the reflection R_{ATB} is negligibly small. However, if one choose a smaller G and a larger injection angle α, R_{ATB} is finite [27]. In this latter case, both types of Andreev reflections, R_{ATB} and R_{ATT}, may take place simultaneously. This differs from the case of retro- and specular-Andreev reflections in SM with Dirac spectrum, where one or the other is finite by crossing the charge neutrality point [22,29,30].

To make a connection with possible transport experiments, we now turn the focus upon the differential conductance (DC), which is a quantity accessible in conventional transport experiments. For this purpose, we assume that the two left normal contacts are placed at the same potential V and that the two right superconducting contacts are grounded. The DC can be expressed in terms of the

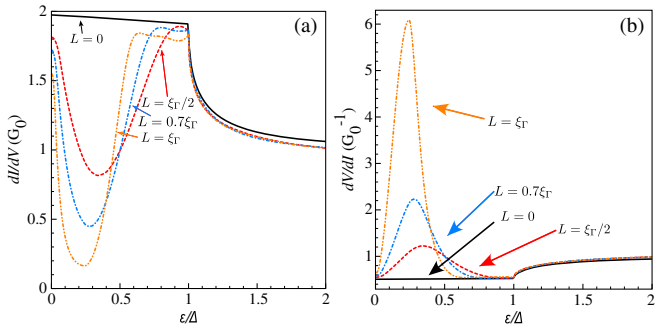

FIG. 3. (a) Differential conductance as a function of the applied bias and for different lengths L of the EC region, the various lines correspond to $\Gamma = 1$, $\Delta = 4\Gamma$, $G = 100\Gamma$ and $H_L = H_R = 0$. (b) Differential resistance as a function of the applied bias and different length of the EC region. In the figure we have set $\Gamma = 1$, $\Delta = 12\Gamma$, $G = 60\Gamma$ and $H_{SM-EC} = H_{EC-SSM} = 0.5$, The parameters are chosen in accordance to Ref. [9,32]. In both panels, the different lines refer to $L = 0$ (black solid line), $L = \xi_\Gamma/2$ (red dashed line), $L = 0.7\xi_\Gamma$ (blue dashed-dotted line), and $L = \xi_\Gamma$ (orange dashed-dashed-dotted-dotted line).

reflection probabilities (5) by using a generalized expression based on the Blonder-Tinkham-Klapwijk formula [25,31],

$$\frac{\partial I}{\partial V} = G_0(eV)\int_0^{\pi/2}\sum_{\beta\in\{T,B\}}[1 - R_{NT\beta}(eV,\alpha) + R_{AT\beta}(eV,\alpha)]\cos\alpha d\alpha. \quad (7)$$

Here $G_0(eV)$ is the differential conductance of the normal state.

Figure 3(a) shows the DC as a function of the injection energy, which is proportional to the applied voltage, and for different values of the length L. Notice first that the DC is not equal to $2G_0$ for $L = 0$. This is a consequence of considering a finite chemical potential [22]. For a finite-length EC region the DC decreases faster as a function of the voltage; it reaches a minimum and then increases up to a voltage of the order of Δ. It is also worth to notice that the DC of the normal state in the presence of a finite EC is also smaller compared to the case without it.

The decrease of the DC is due to a normal reflection channel that accounts for electrons injected from the TL and reflected into the BL. Thus, the presence of a finite length EC region entirely accounts for the minimum in the DC. If the length L exceeds the decay length ξ_Γ, injected electrons with $E < \Gamma$ rarely reach the superconducting electrode (cf. Fig. 2) and, therefore, the DC remains small up to voltages of the order $|\Gamma|$ [18].

We can obtain an analytical expression for the low- bias behavior of the DC in the short-junction limit, using Eqs. (6), and within the Andreev approximation,

$$\frac{dI}{dV} = G_0\left(1 - 8\delta^2\frac{(eV)^2\Gamma^2}{\Delta^2[\Gamma^2 - (eV)^2]}\right). \quad (8)$$

According to this expression, the low-voltage peak in the DC is of the order of Γ. This suggests that transport measurement using superconducting electrodes could be used to directly estimate the size of the order parameter Γ.

Our results for the differential conductance may help to understand measurements of the differential resistance of a superconductor–HgTe-quantum-well junction. The quantum well has a width of 20 nm [9]. One of the most striking findings in this experiment is a zero-bias peak in the measured differential resistance [9] that can be seen as the manifestation of an EC gap. Indeed, in light of our model, the size of the zero-bias peak corresponds to the EC gap. This comparison is shown in Fig. 3(b), where we plot the differential resistance by choosing parameters consistent with the experiments on HgTe quantum wells [9,32]. Although the agreement between theory and experiment looks promising we would like to be cautious at this point because our approach assumes a full ballistic system, whereas the samples measured in Ref. [9] have a size of several μm and disorder might play a role [33]. Further experiments and analysis are needed to draw definite conclusions.

Conclusions.—We have studied the electronic transport through an electron-hole bilayer in contact with normal and superconducting electrodes. We have assumed that the electron-hole bilayer hosts an exciton condensate. The transport properties of this junction are determined by the competition of different coherent reflection processes occurring at the interfaces with the normal and superconducting electrodes. As a consequence of this competition, the differential conductance has a minimum at voltages of the order Γ/e, where Γ is the EC order parameter. The observation of this minimum in an electron-hole bilayer system represents a unique hallmark of the presence of the EC. Good candidates for our proposal are double bilayer-graphene systems separated by hexagonal boron nitrate [13,14]. In bilayer graphene, superconductivity induced by proximity effect has been already observed [29]. Moreover, from our model one might interpret the zero-bias peak observed in the differential resistance of a HgTe quantum-well–superconductor junction as a manifestation of an EC phase.

Discussions with B. Bujnowski, E. Deviatov, F. Konschelle, V. Golovach, T. T. Heikkilä, P. Lucignano, M. Rontani, and T. van den Berg are acknowledged. The work of D. B. and F. S. B. is supported by Spanish Ministerio de Economía y Competitividad (MINECO) through the Project No. FIS2014-55987-P and by the Transnational Common Laboratory *QuantumChemPhys*. T. M. K. acknowledges the financial support from the European Research Council Advanced Grant No. 339306 (METIQUM), and the Ministry of Education and Science of the Russian Federation, Contract No. 14.B25.31.0007.

*dario.bercioux@dipc.org
†sebastian_bergeret@ehu.eus

[1] L. V. Keldysh and Y. Kopaev, Fiz. Tverd. Tela **6**, 2791 (1965) [Sov. Phys. Solid State **6**, 2219 (1965)].
[2] D. Jérome, T. M. Rice, and W. Kohn, Phys. Rev. **158**, 462 (1967).
[3] M. Combescot and S.-Y. Shiau, *Excitons and Cooper Pairs: Two Composite Bosons in Many-Body Physics* (Oxford University Press, United Kingdom, 2016).
[4] B. I. Halperin and T. M. Rice, Rev. Mod. Phys. **40**, 755 (1968).
[5] C. Monney, E. F. Schwier, M. G. Garnier, N. Mariotti, C. Didiot, H. Cercellier, J. Marcus, H. Berger, A. N. Titov, H. Beck *et al.*, New J. Phys. **12**, 125019 (2010).
[6] K. Rossnagel, J. Phys. Condens. Matter **23**, 213001 (2011).
[7] G. M. Minkov, A. V. Germanenko, O. E. Rut, A. A. Sherstobitov, S. A. Dvoretski, and N. N. Mikhailov, Phys. Rev. B **88**, 155306 (2013).
[8] M. Knap, J. D. Sau, B. I. Halperin, and E. Demler, Phys. Rev. Lett. **113**, 186801 (2014).
[9] A. Kononov, S. V. Egorov, Z. D. Kvon, N. N. Mikhailov, S. A. Dvoretsky, and E. V. Deviatov, Phys. Rev. B **93**, 041303 (2016).
[10] J. Kasprzak, M. Richard, S. Kundermann, A. Baas, P. Jeambrun, J. M. J. Keeling, F. M. Marchetti, M. H. Szymańska, R. André, J. L. Staehli *et al.*, Nature (London) **443**, 409 (2006).
[11] A. F. Croxall, K. Das Gupta, C. A. Nicoll, M. Thangaraj, H. E. Beere, I. Farrer, D. A. Ritchie, and M. Pepper, Phys. Rev. Lett. **101**, 246801 (2008).
[12] J. A. Seamons, C. P. Morath, J. L. Reno, and M. P. Lilly, Phys. Rev. Lett. **102**, 026804 (2009).
[13] J. I. A. Li, T. Taniguchi, K. Watanabe, J. Hone, A. Levchenko, and C. R. Dean, Phys. Rev. Lett. **117**, 046802 (2016).
[14] K. Lee, J. Xue, D. C. Dillen, K. Watanabe, T. Taniguchi, and E. Tutuc, Phys. Rev. Lett. **117**, 046803 (2016).
[15] M. M. Fogler, L. V. Butov, and K. S. Novoselov, Nat. Commun. **5**, 521 (2014).
[16] E. V. Calman, C. J. Dorow, M. M. Fogler, L. V. Butov, S. Hu, A. Mishchenko, and A. K. Geim, Appl. Phys. Lett. **108**, 101901 (2016).
[17] G. Vignale and A. H. MacDonald, Phys. Rev. Lett. **76**, 2786 (1996).
[18] M. Rontani and L. J. Sham, Solid State Commun. **134**, 89 (2005).
[19] M. Rontani and L. J. Sham, Phys. Rev. Lett. **94**, 186404 (2005).
[20] B. Wang, J. Peng, D. Y. Xing, and J. Wang, Phys. Rev. Lett. **95**, 086608 (2005).
[21] X. Zhu, P. B. Littlewood, M. S. Hybertsen, and T. M. Rice, Phys. Rev. Lett. **74**, 1633 (1995).
[22] C. W. J. Beenakker, Phys. Rev. Lett. **97**, 067007 (2006).
[23] F. Dolcini, D. Rainis, F. Taddei, M. Polini, R. Fazio, and A. H. MacDonald, Phys. Rev. Lett. **104**, 027004 (2010).
[24] S. Peotta, M. Gibertini, F. Dolcini, F. Taddei, M. Polini, L. B. Ioffe, R. Fazio, and A. H. MacDonald, Phys. Rev. B **84**, 184528 (2011).
[25] G. E. Blonder, M. Tinkham, and T. M. Klapwijk, Phys. Rev. B **25**, 4515 (1982).
[26] The use of the Blonder-Tinkham-Klapwijk formalism assumes a sharp boundary between the different regions, in particular, an abrupt change of the superconducting pair correlations at the SSM-EC interface. This assumption is well justified if the size of the contact between the two regions is much smaller than its lateral dimensions. This condition can be achieved experimentally by proper design of the contact. However, even in the case of a smooth transition of the pair correlations at the interface, and we expect to have qualitatively similar results.
[27] See Supplemental Material at http://link.aps.org/supplemental/10.1103/PhysRevLett.119.067001 for full details of the calculations, which includes Ref. [28].
[28] D. Averin and A. Bardas, Phys. Rev. Lett. **75**, 1831 (1995).
[29] D. K. Efetov, L. Wang, C. Handschin, K. B. Efetov, and J. Shuang, Nat. Phys. **12**, 328 (2015).
[30] W. Chen, L. Jiang, R. Shen, L. Sheng, B. G. Wang, and D. Y. Xing, Europhys. Lett. **103**, 27006 (2013).
[31] N. A. Mortensen, K. Flensberg, and A.-P. Jauho, Phys. Rev. B **59**, 10176 (1999).
[32] Z. D. Kvon, E. B. Olshanetsky, E. G. Novik, D. A. Kozlov, N. N. Mikhailov, I. O. Parm, and S. A. Dvortsky, Phys. Rev. B **83**, 193304 (2011).
[33] See Supplemental Material at http://link.aps.org/supplemental/10.1103/PhysRevLett.119.067001 for a more detailed comparison of or results with those of the experiment of Ref. [9].